

Paradoxical effects of a stress signal on pro- and anti-apoptotic machinery in HTLV-1 Tax expressing cells

Cynthia de la Fuente,⁴ Lai Wang,⁴ Dai Wang,⁴ Longwen Deng,⁴ Kaili Wu,⁴ Hong Li,¹ Dana Stein,³ Thomas Denny,³ Frederick Coffman,² Kylee Kehn,⁴ Shanese Baylor,⁴ Anil Maddukuri,⁴ Anne Pumfery⁴ and Fatah Kashanchi⁴

¹Department of Biochemistry and Molecular Biology; ²Department of Pathology; ³Department of Pediatrics, UMDNJ-New Jersey Medical School, Newark, NJ; ⁴Department of Biochemistry and Molecular Biology, George Washington University, Washington DC, USA

Received 17 June 2002; accepted 27 August 2002

Abstract

Adult T-cell leukemia (ATL) and HTLV-1 associated myelopathy/tropical spastic paraparesis (HAM/TSP) are associated with Human T-cell lymphotropic virus type 1 (HTLV-1) infection. The viral transactivator, Tax is able to mediate the cell cycle progression by targeting key regulators of the cell cycle such as p21/waf1, p16/ink4a, p53, cyclins D₁₋₃/cdk complexes, and the mitotic spindle checkpoint MAD apparatus, thereby deregulating cellular DNA damage and checkpoint control.

Genome expression profiling of infected cells exemplified by the development of DNA microarrays represents a major advance in genome-wide functional analysis. Utilizing cDNA microarray analysis, we have observed an apparent opposing and paradoxical regulatory network of host cell gene expression upon the introduction of DNA damage stress signal. We find the apparent induction of cell cycle inhibitors, and pro- as well as anti-apoptotic gene expression is directly linked to whether cells are at either G1, S, or G2/M phases of the cell cycle. Specifically, a G1/S block is induced by p21/waf1 and p16/ink4a, while pro-apoptotic expression at S, and G2/M is associated with caspase activation, and anti-apoptotic gene expression is associated with up regulation of Bcl-2 family member, namely *bfl-1* gene. Therefore, the microarray results indicating expression of both pro- and anti-apoptotic genes could easily be explained by the particular stage of the cell cycle. Mechanism and the functional outcome of induction for both pathways are discussed. (*Mol Cell Biochem* **245**: 99–113, 2003)

Key words: HTLV, Tax, cell cycle, transcription, apoptosis, microarray

Introduction

Genome expression profiling exemplified by the development of DNA microarrays represents a major advance in genome-wide functional analysis [1, 2]. Using a single assay, the transcriptional response of each gene to a change in its cellular state can be measured, whether it is a viral infection, host cell

cycle changes, chemical treatment, or genetic perturbation. Specifically, systematic approaches for identifying the biological functions of cellular genes altered during changes such as viral infection, are needed to ensure rapid progress in defining significant genome sequences in directed experimentation and applications.

Utilizing a number of microarray procedures from various

retrovirally infected cells, we have recently observed an apparent opposing and paradoxical regulatory network of host cell gene expression upon the introduction of stress signals. Specifically, we have observed induction of both pro- and anti- apoptotic genes in cells that express viral activators. Induction of these cellular host genes is enhanced upon introduction of stress signals, such as gamma irradiation. Here, as a proof of principal, we describe the effects of a viral activator that controls both host cell cycle checkpoints [3–13], apoptotic machinery [14–26], and show how cells at various stages of the cell cycle induce an opposing pro- or anti-apoptotic effect upon stress.

Adult T-cell leukemia (ATL) and HTLV-1 associated myelopathy/tropical spastic paraparesis (HAM/TSP) are associated with human T-cell lymphotropic virus type 1 (HTLV-1) infection (reviewed in [27]). The viral transactivator Tax is able to mediate the cell cycle progression by targeting key regulators of the cell cycle such as p21/waf1, p16/ink4a, p53, cyclins D₁₋₃/cdk complexes, and the mitotic spindle checkpoint apparatus [3–13, 28], thereby deregulating cellular DNA damage and checkpoint control.

It is widely believed that viral activators control, other than the regulation of transcription, pathways essential to DNA damage checkpoint. Components of the DNA damage detection pathway are integrators, such as tumor suppressor ATM, which coordinates the activities of the recombinational repair processes, and checkpoint/cell cycle inhibitors [29–31]. Cellular checkpoint/cell cycle inhibitors such as Chk1 [32], Chk2 [33], p53 [29], p21/waf1 [29, 34], GADD45 [26], and 14-3-3 [24–29] are upregulated in order to provide sufficient time for repair prior to the critical phases of DNA replication and mitosis. However, loss or alleviation of checkpoints by viral activators may increase spontaneous and induced chromosomal aberrations by reducing DNA repair efficiency or induce apoptosis. Therefore, all three components of the DNA damage surveillance, integrators, repair processes, and cell cycle checkpoints, are targets of viral activators resulting in host genome instability.

We have previously shown that HTLV-1 infected cells arrest at the G1/S boundary when subjected to cellular stress. Upon gamma irradiation, elutriated cells at the early G1 phase were blocked at G1/S, whereas uninfected control cells transgressed into the S phase [3, 4]. Interestingly, we and others [3, 4, 14–18] have also observed HTLV-1 infected cells to undergo increased apoptosis upon cellular stress. Therefore, viral activators such as Tax are capable of stimulating both pro- [14–18] and anti-apoptotic [19–21] pathways. These apparently contradictory findings were also observed in our recent microarray experiments where cells showed both pro- and anti-apoptotic gene expression upon DNA damage. Here we show that (i) When using unsynchronized cells, various pathways including cell cycle inhibitors such as p21/waf1, p16/ink4a, and IL-10; anti-apoptotic genes, such as DAD-1

and Bcl-xL, and pro- apoptotic genes, such as RIP, BAX, MKK3, NIP3, caspase 3, and caspase 10 are all upregulated in Tax expressing cells following DNA damage, (ii) a purified G0/G1 population of Tax expressing clones exhibit a block at G1/S upon introduction of gamma irradiation, whereas a Tax CREB mutant clone was unable to maintain the G1/S block, (iii) purified and gamma irradiated S and G2/M fractionated Tax expressing cells, showed an immense decline of both S and G2/M and an increase in apoptotic cells. This pattern of apoptosis was not seen in the Tax CREB mutant clone, implying that Tax utilizes the CREB/p300/PCAF pathway for both G1/S checkpoint and apoptosis related gene expression.

Materials and methods

Cell culture

C81 (C8166) is a human T-cell lymphocyte virus type 1 infected T-cell line and CEM (12D7) is an uninfected human T-cell line established from patients with T-cell leukemia. C81 cells contain low amounts of viral proteins and do not release virus particles. These cells contain one complete and two deleted proviral genomes [68–70]. Chronic T Lymphocytic Leukemia (CTLL) cells have previously been described [3, 4], which are mouse T-cell lines dependent on IL-2 for their growth. However, upon transfection and selection of the Tax gene, these cells become IL-2 independent. Here, they are designated as CTLL/WT (CTLL cells transfected with wild type Tax) and CTLL/703 (CTLL cells transfected with a CREB Tax mutant, M47). The M47 Tax mutant, has two amino acid substitutions at positions 319 and 320. Both cell types are IL-2 independent. A comparison of Tax expression in C81, WT, and 703 cells has been published previously. C81 and WT cells have similar number of Tax proteins expressed [4, 8]. Human HeLa cells were cultured in Dulbecco's modified Eagle's medium (DMEM) supplemented with 10% Fetal Bovine Serum (FBS), 1% penicillin, streptomycin antibiotics, and 1% L-Glutamine (Quality Biological). All lymphocytes were grown in RPMI-1640 with 10% FBS, 1% streptomycin, penicillin antibiotics, and 1% L-glutamine, and incubated in a 5% CO₂ incubator at 37°C.

cDNA array hybridization

Cells were grown to mid-log phase (5.0×10^6), pelleted and washed twice with cold D-PBS without Ca²⁺/Mg²⁺. Total RNA was extracted on ice using TRIzol Reagent (Life Technologies, Inc.). Purified RNA was analyzed on a 1% agarose gel for quality and quantity. Gene expression of HTLV-1 infected C8166 (with and without gamma irradiation treatment)

and uninfected CEM (12D7) was performed as previously described [3, 4], using Atlas Human cDNA Expression Array (Clontech Laboratories Inc., Palo Alto, CA, USA) according to manufacturer's recommendations. In brief, 1 μ g of poly A⁺ RNA each was purified using a CHROMA SPIN-200 column, and reverse transcribed into ³²P-labeled cDNA. The CHROMA SPIN-200 column was used to purify the ³²P-labeled cDNA from unincorporated ³²P-labeled dNTPs and small (< 0.1 kb) cDNA fragments. Each sample was then hybridized to the human cDNA expression array overnight with continuous agitation at 68°C. Next day, the array was washed 3 times with gentle agitation, first wash with 2 \times SSC + 1% SDS and the last 2 washes were with 0.1 \times SSC + 0.5% SDS at 37°C. Arrays were exposed to a PhosphorImager Cassette and analyzed using Molecular Dynamics ImageQuant software.

Gamma-irradiation and flow cytometry

γ -irradiation was performed using a J.L. Shepherd and Associates Mark I Irradiator machine (model 68A utilizing a pair of 6000 Ci ¹³⁷Cs sources in type 6810 capsules). The dosage of irradiation was 7.7 Grays (Gys). To prepare cells for flow cytometric analysis, samples were centrifuged at 3,000 rpm in a Sorvall RT 6,000 at 4°C for 5 min. Cell pellets were washed twice with D-PBS without Ca²⁺/Mg²⁺ and centrifuged. Cell pellets were then resuspended in 70% ethanol and kept at 4°C. Once all samples were collected, they were then centrifuged at 3,000 rpm at 4°C for 10 min. Cell pellets were re-hydrated on ice for 15 min with D-PBS without Ca²⁺/Mg²⁺. Cells were pelleted and resuspended in 1 ml of propidium iodide (PI) staining solution (50 μ g/ml propidium iodide, 10 μ g/ml RNase A, 0.1% NP-40, D-PBS with Ca²⁺/Mg²⁺). Samples were then subjected to flow cytometry using a Becton Dickinson FACS Caliber with a 488-nm argon laser. Acquisition was done using CELLQuest software (Becton Dickinson) and analysis was performed with ModFit LT software (Verity Software House, Inc.).

Centrifugal elutriation

CTLL/WT and CTLL/703 cultures were grown and harvested at log phase of growth (total of 1 \times 10⁹). Cultures were washed once with D-PBS without Ca²⁺/Mg²⁺ and 3 mM EDTA, pH 7.5 (elutriation buffer), and resuspended in the same buffer. A Beckman J6-MI elutriation rotor was washed with 70% ethanol followed by elutriation buffer and then the rotor was brought to 2700 rpm and 18°C. Cells were loaded at 18 ml/min and 150-ml fractions were collected at flow rates of 23, 27, 30, 38, 45, 50, and 70 ml/min. Fractions were washed once, centrifuged, resuspended with D-PBS with Ca²⁺/Mg²⁺, and divided equally for 0 and 24 h samples (\pm γ -irradiation).

The zero hour fraction aliquots were processed and placed in 70% ethanol for FACS analysis. The γ -irradiated-24 h samples were placed in complete media, γ -irradiated with a 770 Rads, and cultured for 24 h at 37°C. All samples were further processed for FACS analysis using propidium iodide staining.

Transient transfection assays

Lymphocytes (CEM [12D7]) were grown to the mid-log phase of growth in complete RPMI-1640 medium. Cells were co-transfected with various plasmid DNAs, including wild type Tax (WT), Tax (M47), Tax (M22), Bfl-1 CAT, Bfl-1 mkB CAT, and pU₃R-CAT (HTLV-LTR-CAT) using electroporation [8] and harvested for CAT assay 18 h following transfection. HeLa cells were transfected with either pCMV-*bfl-1* (15 μ g) or an empty pCMV vector as a control using electroporation. Cells were plated into 100-mm plates with complete DMEM medium. After 24 h, cells were treated with either cyclohexamide alone (10 μ g/mL) or together with γ -irradiation (770 Rads). At day 5, the media was removed and cells were washed with PBS, stained with 2 ml of 0.4% Trypan Blue, and counted for cell survival.

Mass spectrometry

The in-gel digestion was performed based on a procedure previously described by Fernandez *et al.* [35]. The gel bands of interest were excised from a 4–20% Tris glycine SDS-PAGE and digested overnight at 37°C with 0.2 μ g of trypsin (Promega, modified sequencing grade trypsin). Digested samples were desalted using C₁₈ ZipTips (Millipore) according to the manufacturer's protocol. A 1 μ l aliquot of sample was taken for peptide mass mapping on a PerSeptive Biosystem DEPRO MALDI-TOF Mass Spectrometer using α -cyano-4-hydroxycinnamic acid as the matrix. Analysis was performed in the linear delayed-extraction mode with external calibration. Protein identification by mass mapping was performed through the program available from the University of California at San Francisco (<http://rafael.ucsf.edu/cgi-bin/msfit>), the ProFound program at the Rockefeller University (<http://prowl.rockefeller.edu/cgi-bin/ProFound>), the PepSearch program at the EMBL in Heidelberg (http://www.mann.embl-heidelberg.de/Services/PeptideSearch/FR_peptideSearchForm.html), Mascot (www.matrixscience.com), and TagIdent available on the ExPASy World Wide Web server.

Immunoprecipitations and immunoblotting

Extracts and immunoprecipitations were performed as previously described [3, 4]. Amounts of extracts used are as

noted in figure legends. Antibodies used were α -p21/waf1 (C-19), α -Bax (N-20), α -p16/ink4a (N-20), α -PARP (N-20), α -Caspase 3 (H-277) from Santa Cruz Biotech, α -14-3-3 τ/θ (Ab-1) from Calbiochem, and α -Tax1 (generous gift of Dr. S. Gitlin).

RNase protection assay

The RNase Protection Assay (RPA) was performed using the RiboQuantTM RPA kit (BD Pharmingen, San Diego, CA, USA) with two multi-probe mouse template sets (mAPO-1 and mAPO-2). Assays were performed according to manufacturer's recommendations using RNA from CTLL/WT and CTLL/703 cells with and without irradiation treatment.

Results

Expression of cell cycle blockers, pro- and anti-apoptotic genes in HTLV-1 infected T cells

We and others have previously observed that HTLV-1 infected cells undergo increased apoptosis upon cellular stress [14–21, 28]. To determine the mechanism, we initially investigated the overall expression of cellular mRNAs in HTLV-1 infected cells by utilizing human cDNA expression arrays (Clontech, 588 genes). As seen in Fig. 1A, various pathways including cell cycle inhibitors, such as p21/waf1, p16/ink4a, and IL-10, were upregulated in HTLV-1 infected, Tax expressing, T cells. Also both anti-apoptotic genes, such as DAD-1 and Bcl-xL, and pro-apoptotic genes, such as RIP, BAX, MKK3, NIP3, caspase 3, and caspase 10 (C81 vs. CEM column) were up regulated in Tax expressing cells. Using stringent wash conditions, induced expression of these genes in infected cells ranged anywhere from 1.2–2.0 fold over that of the uninfected CEM control cells. Similar regulation of these genes have also been previously reported [3, 4, 36].

Interestingly, γ -irradiation of Tax expressing cells (γ -C81 vs. C81) showed a further increase of cdk inhibitors, such as p16/ink4a, and pro-apoptotic genes, such as caspase 10. A FACS histogram of the cells before and after irradiation revealed an increase in the G1 as well as apoptotic cells [data not shown, 3, 4]. It was also noted that the cDNA filter arrays used here could not distinguish between p16/ink4a and p19/ink4d since both sequences are derived from the same region of these two genes and printed as unspliced cDNAs on the filters. We therefore performed Western blots to distinguish between the two cdk inhibitors and further confirmed results obtained from the microarray experiments. A collective sample of gene products detected by Western blot is shown in Fig. 1B, where upregulation of p16/ink4a, p21/waf1, and Bax was observed from the Tax expressing cells.

A)

Genes	Functional Pathway	C81 vs. CEM	γ -C81 vs. C81
p21/Waf1	G1/S Blocker	1.2	1.3
p16/p19INK4d	G1/S Blocker	1.2	2.6
IL-10	G1/S Blocker	1.9	2.9
RIP	Pro-Apoptosis	2	1.8
Bax	Pro-Apoptosis	1.2	1.6
NIP3	Pro-Apoptosis	0.9	1.6
MKK3	Pro-Apoptosis	1.4	1.7
Caspase 3	Pro-Apoptosis	1.6	1.7
Caspase 10	Pro-Apoptosis	2	3
DAD-1	Anti-Apoptosis	2	1.7
BCL-XL	Anti-Apoptosis	2	2
GAPDH	Housekeeping	0.9	0.9
Ubiquitin	Housekeeping	1	1.3

B)

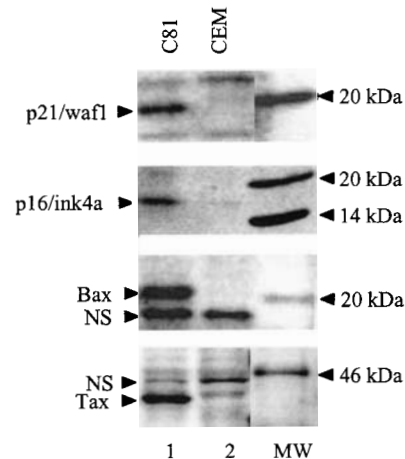


Fig. 1. Comparison of cell cycle, pro-, and anti-apoptotic genes in HTLV-1 infected and uninfected T-cells. (A) Gene expression of uninfected (CEM [12D7]) and HTLV-1 infected (C81) T-cells treated with or without gamma irradiation, were performed using the Human Atlas cDNA Expression Array (588 genes, Clontech, USA). ImageQuant software was used to obtain actual counts from blots. In comparing cDNA blots we correlated house-keeping genes ubiquitin and glyceraldehyde 3-phosphate dehydrogenase (GAPDH) as controls for normalizing the data. The normalized counts were then used to calculate the fold induction for each gene of interest. Name, functional pathway, and fold induction for selected genes are listed. (B) Comparison of cell cycle, pro-, and anti-apoptotic protein expression in HTLV-1 Infected T-cells. Western blot analysis from CEM and C81 (IL-2 independent) were performed using 50-microgram quantities of whole-cell extracts, loaded onto a Tris-Glycine 4–20% polyacrylamide gel (Invitrogen), transferred to a PVDF membrane, and Western blotted with either α -p21/waf1 rabbit polyclonal Ab, α -Tax rabbit polyclonal Ab, α -p16/ink4a rabbit polyclonal Ab, or α -Bax rabbit polyclonal Ab. Lane 1 contains C81 (HTLV-1 infected T-cell) and lane 2 contains CEM (uninfected) extracts.

Induction of cell cycle block and apoptosis in Tax expressing cells

To examine the possible effects of Tax on pro- and anti-apoptotic pathways, we utilized centrifugal elutriation of a Tax+ clone, CTLL/WT (WT) and a CREB mutant Tax clone, CTLL/703 (703). Both clones express similar levels of Tax protein as judged from western blots [data not shown, 3, 4]. Figures 2A and 2B (top panels) depicts the flow cytometric analysis of WT and 703 cells before and after γ -irradiation. γ -Irradiation of either unsynchronized or elutriated G0/G1, S, and G2/M cell populations was performed. Irradiation of either unsynchronized cell types resulted in a similar FACS profile, except there was an appearance of an apoptotic peak only in WT and not in 703 cells after 24 h of treatment (WT cells, sub G₁, 27.14% vs. 703 cells, sub G₁, 0%).

However, a more interesting set of results emerged when using elutriated cells. Similar to our previous results with human HTLV-1 infected T-cells [3,4], a primarily G0/G1 population of the Tax+ clone (WT) were blocked at G1/S upon exposure to γ -irradiation (89.80 vs. 83.28%). Interestingly, the CREB mutant, 703, was unable to maintain a G1/S block (82.06 vs. 29.71%) and traversed into the S (15.87 vs. 42.92%) and G2/M (2.08 vs. 27.92%) phases without any apparent apoptosis. The ability of wildtype, but not a mutant Tax cell line, to maintain a G1/S block may be attributed to the observed increase of p21/waf1 cdk inhibitor, which associates with cyclin A/cdk2 [3, 4], and/or increased expression of p16/ink4a cdk inhibitor, which regulates Rb phosphorylation [37].

Upon γ -irradiation of S and G2/M fractionated WT cells, an immense decline of both S and G2/M populations (S: 76.68 vs. 16.92%, G2/M: 60.95 vs. 9.94%) and an increase in apoptotic cells (from S fraction: 0 vs. 50.17%, from G2/M fraction: 0 vs. 23.38%) were observed. In dramatic contrast, irradiation of 703 purified fractions, showed no G1/S block or apoptosis, as was evident in the G0/G1 (82.06 vs. 29.17%) and S fractions (73.64 vs. 35.44%, Fig. 2B). A transient block of the G2/M population in 703 cells was observed (73.73 vs. 65.71%), where cells eventually traversed into the G1 phase 12 h later (data not shown). More importantly, we observed no apoptosis from any of the G0/G1, S, or G2/M populations in 703 cells. Collectively, these results imply that the Tax/CREB/PCAF interaction/pathway, as present in the WT cells, is important for both the G1/S checkpoint, by increasing the expression of G1/S blockers such as cdk inhibitors p21/waf1 [3, 4] p16/ink4a, and IL-10 [38], as well as the S and G2/M mediated apoptosis, as evident in the induction of pro-apoptotic genes [39].

For the pro-apoptotic pathway, we next examined the DNA damage surveillance network markers such as poly (ADP-ribose) polymerase (PARP), a zinc-finger DNA binding protein that detects and signals DNA strand breaks [22, 23].

Studies using knock-out animal data and various inhibitors have shown that PARP plays a key role in DNA base excision repair (BER) and execution of programmed cell death by negatively regulating Ca²⁺/Mg²⁺-dependent endonucleases (CME) [40–42]. To further investigate the apoptosis observed in the S and G2/M fractions of WT cells, we examined the status of PARP in WT elutriated cells. We used MOLT-4 cells as a positive control cell line (containing wild type p53) which are readily apoptosed upon irradiation [43]. Results of such an experiment is shown in Fig. 2C, where each of the WT fractions S, S/G2, and G2/M, revealed degradation of PARP, similar to that observed in the MOLT-4 cells. PARP has been shown to be a common downstream substrate for the cysteine protease CED-3/CPP32 subfamily member, caspase 3. Western blot for caspase-3 in WT Tax expressing cells showed an increase in the pro-caspase-3 protein in the S, S/G2, and G2/M fractions upon gamma irradiation (Fig. 2C, second panel), implying that the apparent apoptosis in these fractions may be related to an increase in caspase protein levels and subsequent PARP cleavage.

Loss of G2/M checkpoint and apoptosis

To define the initial and upstream signal for the pro-apoptotic pathway in the S and G2 stages in WT cells, we focused on the G2/M checkpoint protein, 14-3-3. 14-3-3 proteins are highly conserved family members found in yeast, plant, and mammalian cells [24]. Ten mammalian isoforms have been discovered: α , β , δ , ϵ , γ , η , τ , θ , σ , and ζ . While α and δ are phosphorylated isoforms of β and ζ , respectively, τ is specific for T lymphocytes, and σ for epithelial cells [24]. Collectively, 14-3-3 members modulate the interactions of signaling cascade proteins, such as Raf, MEK, Bcr-Abl, PKC, c-Abl, and PI-3 kinases, and control G2/M checkpoint by interacting with cdc25, Chk1, Wee1, and cyclinB/cdc2 [24, 25].

We, therefore, decided to examine the levels of 14-3-3 τ under normal and γ -irradiation conditions to determine whether suppression of 14-3-3 protein expression or alternative complexing with other protein partners might explain the lack of a S and G2/M checkpoint in Tax expressing cells. As shown in Figs 3A and 3B, levels of 14-3-3 did not change in either unfractionated or fractionated cells upon gamma irradiation. Since 14-3-3 τ interacting proteins have previously not been defined, we therefore sought to examine interacting partners and whether their binding status to the 14-3-3 protein changed after γ -irradiation. For this we performed immunoprecipitations with anti-14-3-3 antibody, separated proteins on SDS/PAGE and determined polypeptide composition of partners by MALDI-TOF Mass Spectrometry. Immunoprecipitates (IPs) of 14-3-3 τ from CTLL/WT, CTLL/703, and MOLT-4 were run on a 4–20% gradient SDS/PAGE, Coomassie stained, and various reproducible bands were further proc-

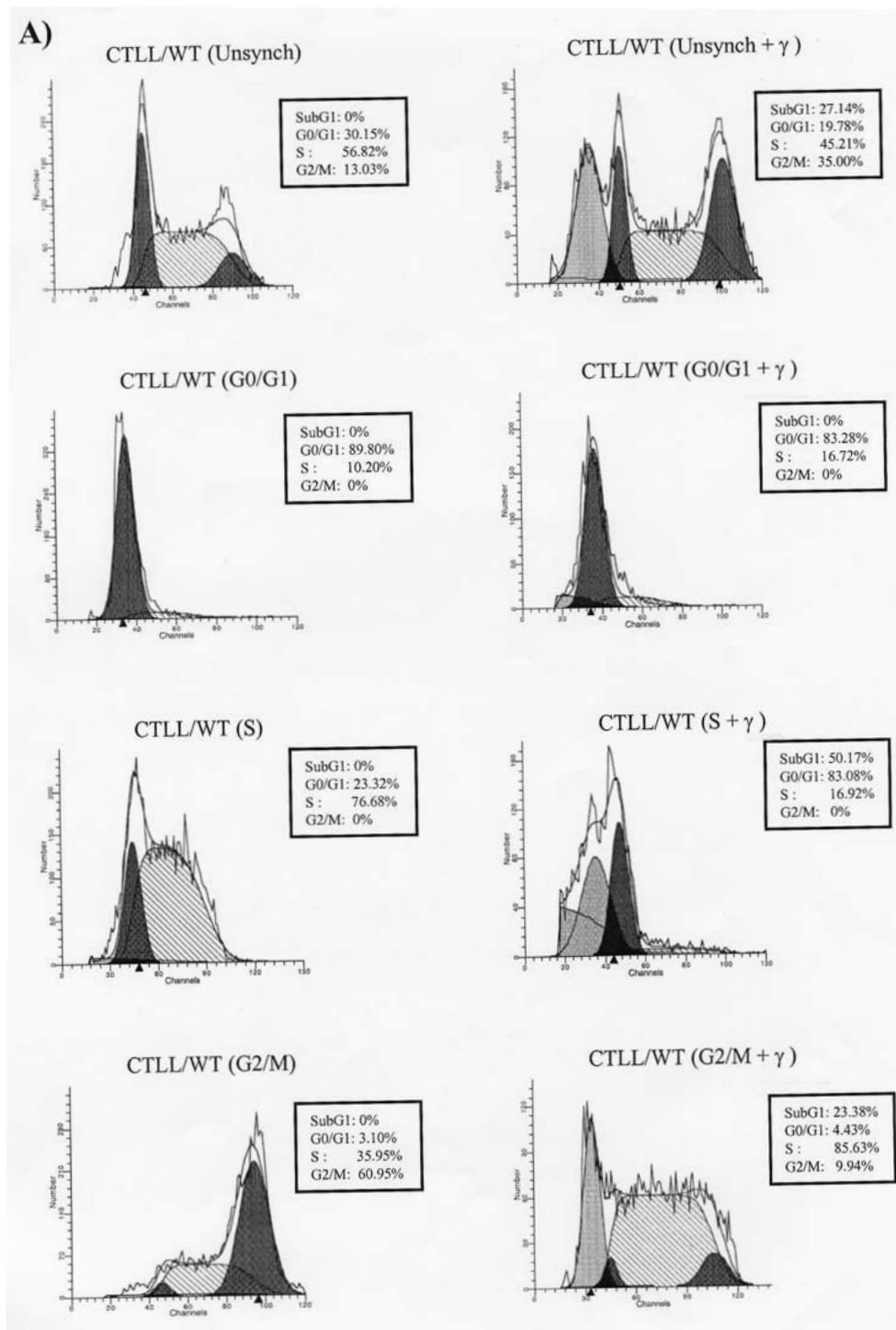


Fig. 2. Effect of γ -irradiation on elutriated cells. Panel A represents CTLL/WT cells and panel B represents CTLL/703 cells which were grown to mid log phase of growth in the absence of exogenous IL-2. Unsynchronised (top panels) and elutriated G0/G1, S, and G2/M fractions were harvested, washed in D-PBS and either directly FACSed at 0 h (left panels) or γ -irradiated and cultured for 24 h prior to FACS analysis (right panels). Each panel depicts cell cycle histogram profiles and percentages of cell numbers at various stages of cell cycle. 'Sub G1' cells represent a collection of cell populations from all stages that were undergoing apoptosis. Panel C (top panel) represents a Western blot of poly(ADP-ribose) polymerase (PARP) from elutriated CTLL /WT cells and unsynchronised MOLT-4. Seventy-five micrograms of whole cell extracts were loaded onto a 4–20% Tris Glycine gel (Invitrogen), transferred to a PVDF membrane and Western blotted with α -PARP (N-20) goat polyclonal Ab. Lanes 1 and 2 represents MOLT-4 at 0 h (lane 1) and 24 h following γ -irradiation treatment (lane 2). Lanes 3–8 represent S, S/G2, and G2/M fractions of CTLL/WT with and without γ -irradiation. The lower panel represents a Western blot of Caspase 3 (α -Caspase-3 (H-277) rabbit polyclonal Ab) from elutriated CTLL/WT fractions.

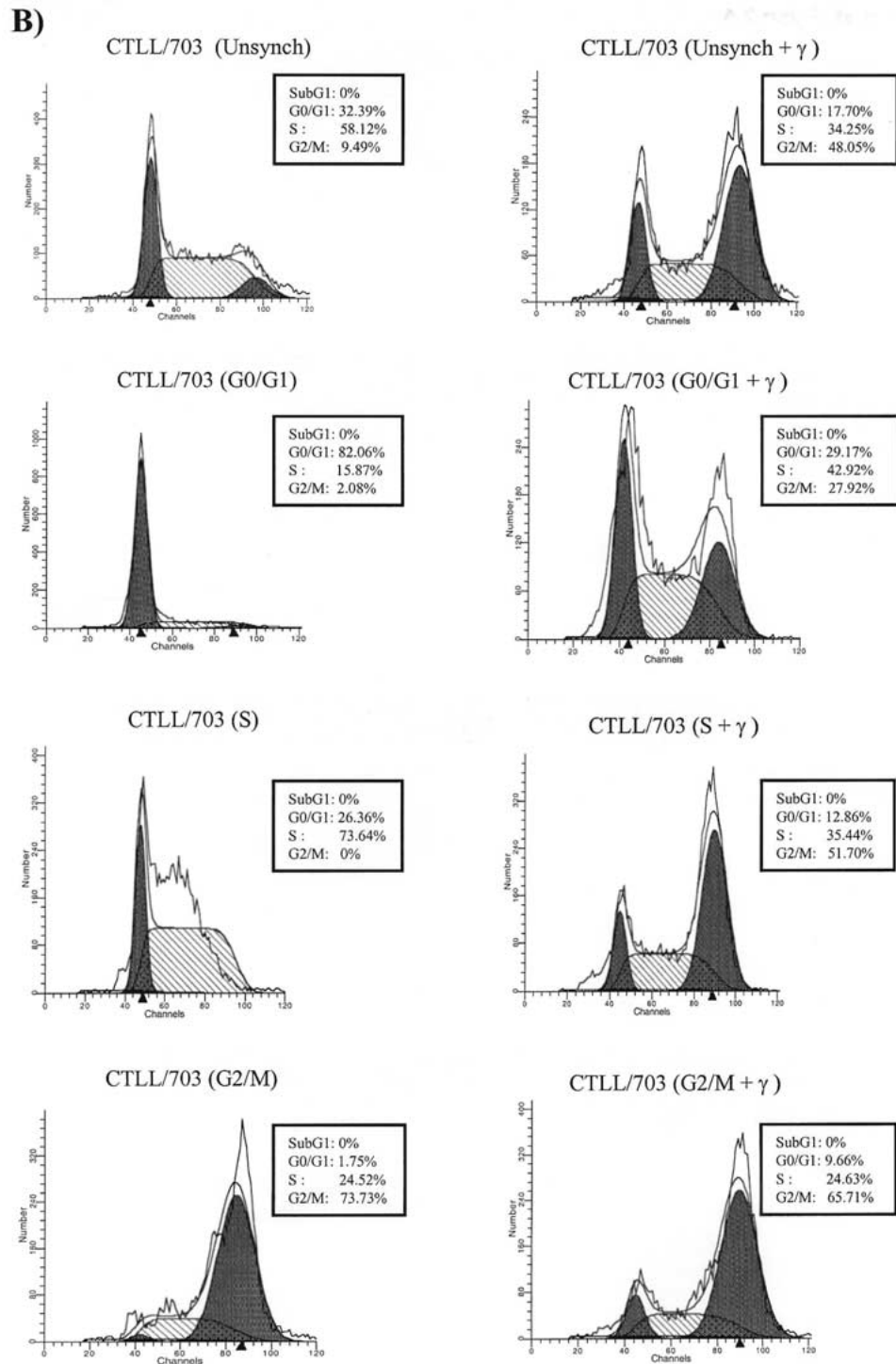


Fig. 2. Continued.

essed. An in-gel digestion of the excised bands with trypsin was performed with each reproducible band and processed for MALDI-TOF MS analysis. Profiles generated from the tryptic digests were determined using databases indicated in

Materials and Methods. Figure 3C represents the Coomassie stained gel from 14-3-3 immunoprecipitations before and after irradiation. Table 1 represents the predicted polypeptide identification of specific bands obtained from SDS/PAGE.

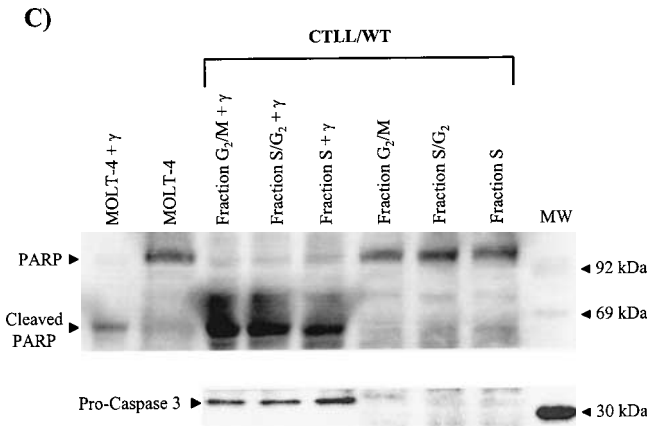


Fig. 2. Continued.

Bands A and B (Fig. 3C, lane 6) were found with high probability to be eukaryotic translation initiation factor 3 subunits 10 (theta) and 9 (eta), respectively. Both bands were decreased after gamma irradiation treatment in the MOLT-4 and WT and not in 703 cells. Translation initiation factors have been known to be regulated at the G₂/M phase by 14-3-3 proteins. Bands C and H were the heavy and light chains from the 14-3-3 antibody. Band D, actin, was a cytoskeletal protein observed in all IPs. Interestingly, bands E, I, and J found in the γ -irradiated MOLT-4 cells (Fig. 3C, lane 6) were determined to be cdc2, Histone 3, and Histone 4, respectively. 14-3-3 τ may directly bind to core histones and alter their phosphorylation and dephosphorylation by PKC [45] and hence modulate the G₂/M checkpoint. Band F was determined to be the 14-3-3 τ wild type protein. A modified version of 14-3-3 τ (lane 6, band G, 28 kDa) was also detected in the γ -irradiated MOLT-4 cells and not in either WT or 703 cells (lanes 1–4, B and F). Collectively, these results imply that the 14-3-3 τ protein is responsible for G₂/M checkpoint control and that the apoptosis effects observed in WT cells is related to the loss of 14-3-3 τ partners.

It is important to note that loss of 14-3-3 partners in MOLT-4 (p53⁺) cells always appeared to be much more rapid than WT (p53⁻) Tax expressing cells. Therefore, we decide to perform our IPs from cells that had been irradiated and cultured for more than the 12 h duration. This is in part due to the hypothesis that there will be a delay in initiation of p53-independent apoptosis after 7.7 Gys of gamma irradiation in WT, but not MOLT-4 cells, combined with the observation that the decrease of G₂/M in WT cells was coupled to an increased percentage of apoptotic cells (data not shown).

Results of an IP from a prolonged irradiation experiment (72 h) is shown in Fig. 3D. Immunoprecipitations from MOLT-4 irradiated cells readily showed a predominant set of only histone proteins complexing with 14-3-3 (lane 4); however, WT Tax expressing cells showed no more than 2–3% of the complex to contain all four histones (lane 2). This

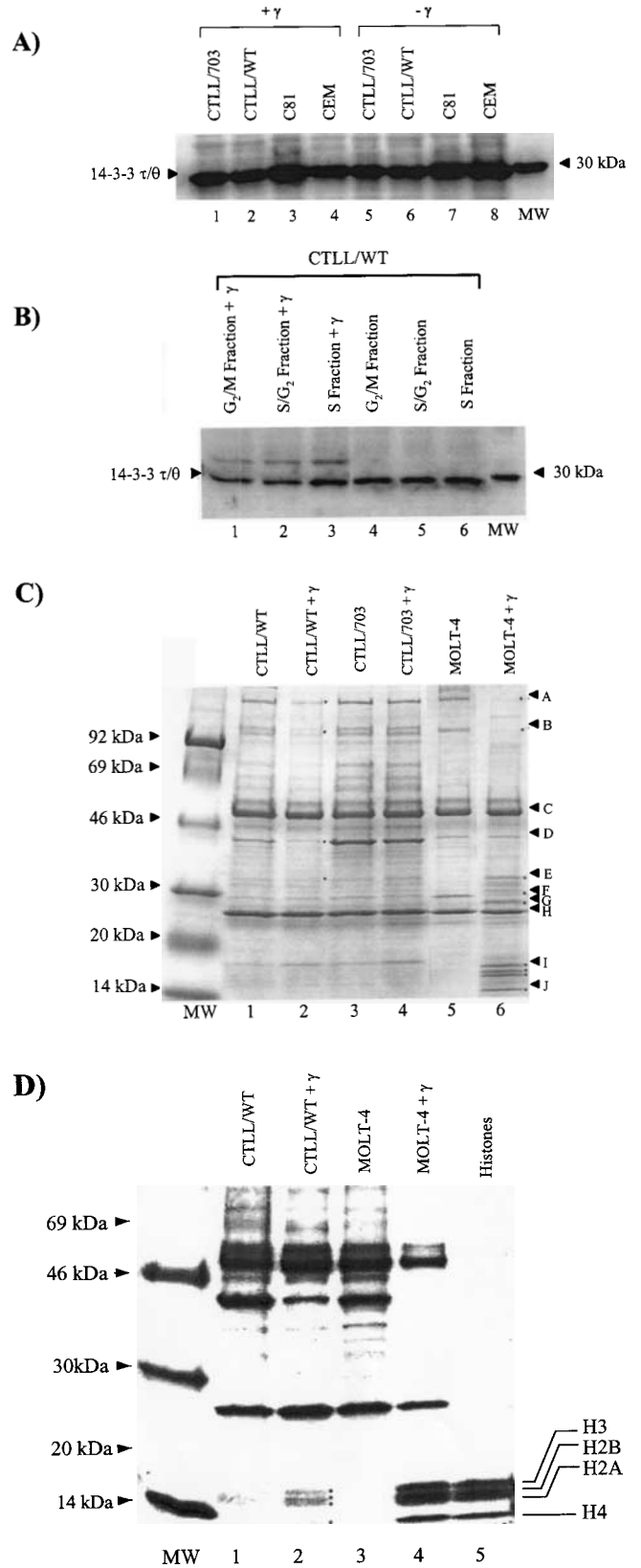


Table 1. MS (MALDI-TOF) suggested proteins from 14-3-3- τ immunoprecipitations

Band	Protein name	NCBI	Theoretical MW	Sequence coverage (%)
A	Eukaryotic translation initiation factor3 subunit 10	6686292	161.93	21
B	Eukaryotic translation initiation factor 3 subunit 9	3123230	92.47	23
C	IgG heavy chain	WB	55.00	WB
D	γ -actin	7441428	41.64	36
E	Cell division cycle 2	4502709	34.08	30
F	14-3-3 τ/θ	WB	28.50	WB
G	14-2-3 τ/θ (cleaved)	5803227	27.75	17
H	IgG light chain	WB	22.00	WB
I	Histone H3	350633	15.24	16
J	Histone H4	3080463	11.22	28

WB – Results from Western blots. The in-gel digestion was performed based on a procedure previously described by Fernandez *et al.* [35]. Analysis was performed in the linear delayed-extraction mode, with external calibration on a PerSeptive Biosystem DEPRO MALDI-TOF Mass Spectrometer. Protein identification by mass mapping was performed through various web sites as indicated in ‘Materials and methods’. The parameters for identification of eIF3, subunits 10 (band A) and 9 (band B) were a monoisotopic tolerance of 75–100 ppm, maximum missed cut of 1 and 2, and partial methionine oxidation. For the mass fingerprinting of Histones H3 (band I) and H4 (band J) a monoisotopic tolerance of 100 ppm, maximum missed cut of 2, and partial methionine oxidation. 14-3-3 τ/θ (band F and G) identification used the following parameters and monoisotopic tolerance of 100 ppm, maximum missed cut of 1, with no modifications.

←

Fig. 3. Expression and functional association of 14-3-3 checkpoint protein. Panel A represents a Western blot of 14-3-3 τ/θ in CEM, C81, CTLL/WT, and CTLL/703 cell lines with and without γ -irradiation treatment. All cultures were grown to mid-log phase of growth and split into two cultures for either untreated or treated with 7.7 Gys for γ -irradiation. Both sets were processed 24 h later. Fifty-micrograms of whole cell extracts were loaded onto a 4–20% Tris Glycine gel (Invitrogen), transferred to a PVDF membrane and western blotted with α -14-3-3 τ/θ mouse monoclonal Ab. Lanes 1–4 represent CTLL/703, CTLL/WT, C81, and CEM, respectively treated with γ -irradiation and 5–8 represented untreated samples. Panel B depicts a Western blot of 14-3-3 τ/θ from cell cycle fractionated CTLL/WT cells that were either untreated or treated with γ -irradiation. Elutriated CTLL/WT S, S/G₂, and G₂/M fractions were washed twice with D-PBS and split in half. One half received 7.7 Gys of γ -irradiation and the other set was untreated. Both sets were harvested 24 h later. Twenty-micrograms of whole cell extracts were loaded onto a 4–20% Tris Glycine gel (Invitrogen), transferred to a PVDF membrane and Western blotted with α -14-3-3 τ/θ mouse monoclonal Ab. Panel C depicts an immunoprecipitations (IP) of 14-3-3 τ/θ from CTLL/WT \pm γ -irradiation CTLL/703 \pm γ -irradiation and MOLT-4 \pm γ -irradiation (as a positive control cell line for apoptosis, γ -irradiation followed by incubation for 12 h prior to IP). One and a half-milligrams of whole cell extracts were IPed with 10 μ l of α -14-3-3 τ/θ mouse monoclonal Ab (Calbiochem). Bound complexes were then washed with TNE 150 + 0.1% NP-40, and then loaded onto a 4–20% Tris Glycine gel and stained with Coomassie Blue. Reproducible bands of interest (highlighted by letters) were then excised, treated with 2 μ g of trypsin for in-gel digestion, and analyzed by MALDI-TOF for mass spectrometry. Lanes 1, 3 and 5 were CTLL/WT, CTLL/703, and MOLT-4 IPs, while lanes 2, 4, and 6 were CTLL/WT + γ , CTLL/703 + γ , and MOLT-4 + γ IPs, respectively. Panel D depicts a similar IP as in panel A, except cells were kept at 37°C for 72 h prior to IP. Dots next to each band represent detectable and reproducible proteins used for mass spec analysis.

suggests that WT (p53⁻) Tax expressing cells apoptose with delayed kinetics from the G2/M boundary, whereas MOLT-4 (p53⁺) cells apoptose readily from the G1/S boundary when treated with 7.7 Gy of γ -irradiation.

Effect of Tax on pro- and anti-apoptotic genes

To directly determine which genes were involved in the pro- and anti-apoptotic machinery, we utilized an RNase Protection Assay (RiboQuant™ RPA kit, BD Pharmingen) with two multi-probe template sets. The left panel of Fig. 4A examines the expression of pro-apoptotic genes (mAPO-1 template), such as caspases 8, 3, and 1. Caspase 1, along with caspase 11, have been shown to be involved primarily in cytokine processing [46]. Caspases 2, 3, and 6–10, are involved in the management and execution of apoptosis [47], and caspase 8 activation (the initiator) is important for subsequent activation of effector caspases, such as caspase 3. While there was a small induction of caspase 8 and 3 expression upon gamma irradiation in the wildtype Tax clones (CTLL/WT vs. CTLL/WT + γ), there was no significant changes in other caspases, including caspase 1.

The right panel of Fig. 4A, is the mAPO-2 template that examines the expression of the Bcl-2 family members, such as Bfl-1, Bcl-xL, and Bcl-2. While there was no significant induction of the anti-apoptotic genes in the wildtype Tax

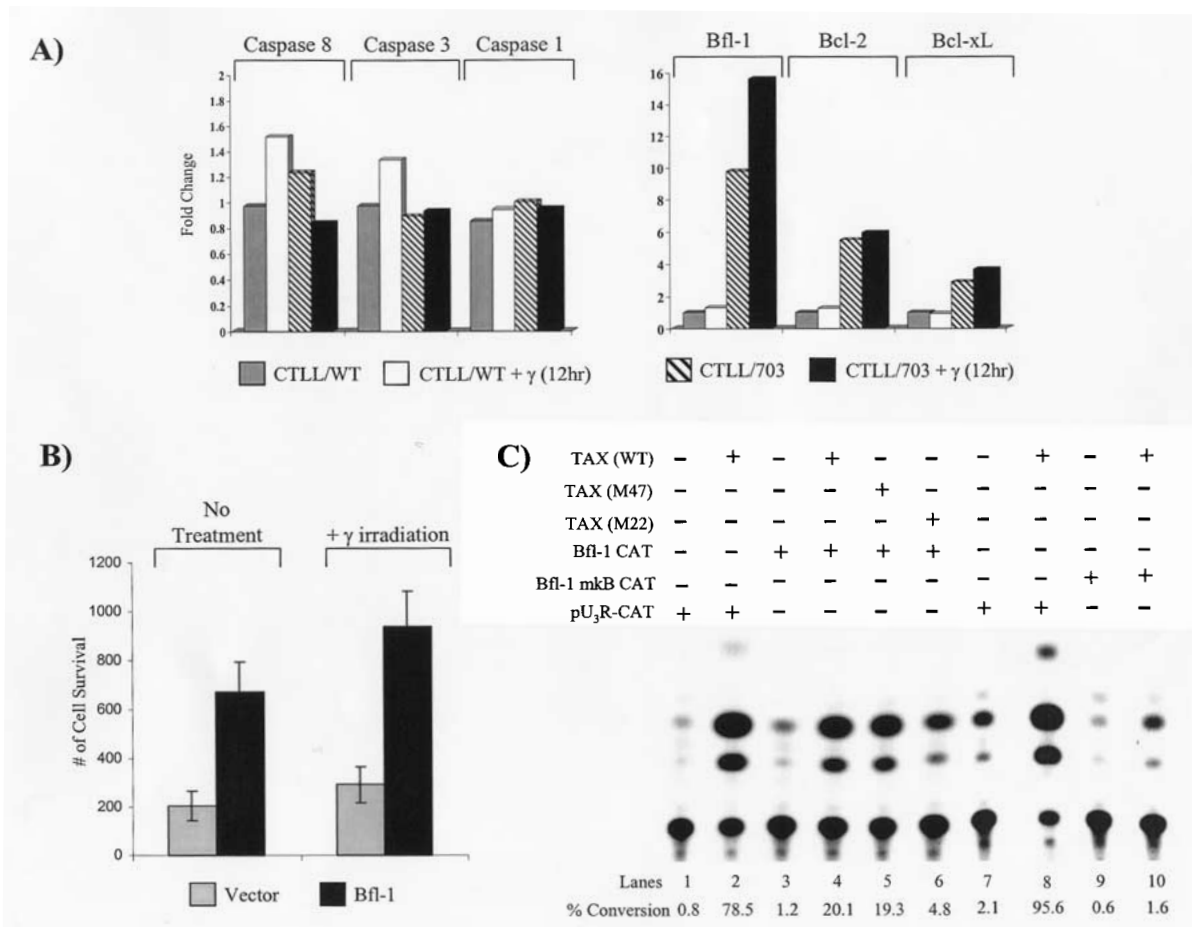


Fig. 4. Transcriptional up-regulation of the pro- and anti-apoptotic machinery in Tax-expressing cells. Panel A depicts counts from a RNase Protection Assay (BD Pharmingen) utilizing CTLL/WT and CTLL/703 RNAs treated either with or without γ -irradiation. All cultures were grown to mid-log phase of growth and split into two and either treated or not with 7.7 Gys of γ -irradiation. Fifteen micrograms of RNA was obtained 12 h after initial treatment and was used for hybridization with various probes. Left panel represents template set mAPO-1 containing pro-apoptotic probes, caspase 8, 3, and 1. Right panel represents template set mAPO-2 containing anti-apoptotic probes, Bfl-1, Bcl-2, and Bcl-xL. Following RNA preparation, hybridization, and digestion with RNases A and T1, protected fragments were separated on a 6% urea-polyacrylamide gel (Invitrogen). Both L32 (cytoplasmic) and GAPDH (nuclear) RNAs were used as controls. Counts and data analysis was obtained using Molecular Dynamics ImageQuant software. Panel B represents cell survival assay following transfection with anti-apoptotic gene *bfl-1*. HeLa cells were transfected with either pCMV-*bfl-1* (15 μ g) or an empty pCMV vector as a control by electroporation. Cells were plated in complete DMEM medium. After 24 h, cells were treated with either Cyclohexamide alone (10 μ g/mL) or together with γ -irradiation (7.7 Gys). At day 5, the media was removed, the cells were washed with PBS, stained with 2 ml of 0.4% Trypan Blue, and counted for cell survival. Data represents the mean \pm S.D. from 3 independent experiments. Panel C represents CAT assays from CEM (12D7) transfected cells. Lanes 1, 2, 7 and 8 are control transfections for basal (pU₃R-CAT, 3 μ g) and activated transcription by Tax (1 μ g). Lanes 3–6 represents CAT assay performed from transfected CEM [12D7] cells with Bfl-1 CAT (6 μ g) and 6 μ g of each Tax plasmid. Lanes 9 and 10 represents transfection of Bfl-1 mkB CAT (Mutation at NF κ B sites in the Bfl-1 promoter, 10 μ g) alone or with wildtype Tax expression vector (6 μ g). Reaction time for CAT assays were for 1 h for all samples, except lanes 7–10 which were for 24 h.

clone after irradiation (CTLL/WT vs. CTLL/WT + γ); however, there was a 2–8 fold difference in the basal levels of Bcl-xL, Bcl-2, and Bfl-1, between the wildtype and the CREB mutant Tax clone (CTLL/WT vs. CTLL/703).

In mammalian cells, apoptosis can be inhibited by the over-expression of anti-apoptotic members of the Bcl-2 family, including Bcl-2, Bcl-xL, Mcl-1, Bcl-w and Bfl-1/A1. Bfl-1/A1 is the smallest member of the Bcl-2 family and has been shown to retard apoptosis and permit cell proliferation in various cell lines [48]. Chen *et al.* and others have shown that

NF κ B, specifically c-Rel and RelA, were able to directly regulate the expression of the pro-survival factors Bcl-xL and Bfl-1/A1 [49, 50]. When examining for the expression of Bcl-2 family members in both WT and 703 cells, we consistently observed an overall higher expression of anti-apoptotic genes. The higher levels of Bfl-1, Bcl-2, and Bcl-xL in CTLL/703 may be due to a dominance of the Tax/NF κ B pathway and may contribute to the overall expression of Bcl-2 family members resulting in a loss of the G1/S checkpoint and a lack of apoptosis, as observed in Fig. 2B.

We next examined the effects of the Bfl-1 protein and its anti-apoptotic activity in transfected cells. Transient transfection of a CMV-*bfl-1* expression vector plasmid significantly suppressed the γ -irradiation induced killing of HeLa cells in the presence of the protein synthesis inhibitor cyclohexamide (Fig. 4B). Quantitation of cell survival showed that the transient expression of Bfl-1 increased the viability of cells 3–5 fold in comparison to cells transfected with the control pCMV empty vector. This data agrees with the protective effect of Bfl-1 [49] and supports a role for Bfl-1 as a survival factor in irradiation induced signaling pathways that otherwise induces apoptosis.

Previous reports by other colleagues have shown that wildtype Tax and M47 (Tax CREB mutant similar to 703 cells used here) were able to transactivate the Bcl-xL promoter through NF κ B elements [20, 51]. To explore if this was also the case for the *bfl-1* gene, we transfected a Bfl-1 CAT reporter construct, which contains a consensus NF κ B sequence in its promoter, along with expression plasmids encoding either wildtype Tax (Fig. 4B, lane 4), CREB mutant Tax (M47, lane 5), or NF κ B mutant Tax (M22, lane 6) into CEM cells. Only wildtype Tax (WT) and the Tax mutant (M47), which retained the ability to transactivate through NF κ B, were able to transactivate Bfl-1 expression efficiently. To ensure that the induction of expression was due solely to the Tax/NF κ B interaction, we transfected a Bfl-1 mutant NF κ B CAT construct that contained a three base mutation in the NF κ B site [50] along with a Tax (WT) expression plasmid. As seen in Fig. 4C mutation of the NF κ B site resulted in a significant decrease in Bfl-1 transactivation by Tax (lanes 9 and 10).

Discussion

Utilizing a number of microarray procedures and methodologies ranging from cDNA filters (Clontech, Inc.), cDNA and oligonucleotide glass slides (NEN, Inc.), oligonucleotide chip slides (Affymetrix, Inc.), and custom printed arrays, we have consistently observed an apparent opposing and paradoxical regulatory network of host cell gene expression in virally infected cells. This was especially true in retrovirally infected cells including HTLV-1 (presented in the current manuscript), HTLV-II, HIV-1, and SIV. Remarkably, we have observed a consistent pattern of induction of both pro- and anti-apoptotic genes in cells that express viral activators related to human and primate retroviruses.

As seen in HTLV-1 infected cells (Fig. 1), three categories, namely cell cycle blockers (p21/waf1, p16/ink4a, and IL-10), anti-apoptotic genes (DAD-1 and Bcl-xL), and pro-apoptotic genes (RIP, BAX, MKK3, NIP3, caspase 3, and caspase 10), were up regulated in Tax expressing cells. However, these cells don't normally undergo cell cycle blockage

nor apoptose under cell growth conditions. Therefore, we speculate that upregulation of these genes has no apparent functional consequence on normal cell growth *per se*. However, the same genes are further upregulated and show genuine function upon cellular stress (e.g. irradiation). This implies that transcriptional upregulation, as detected with microarray technology, has to reach a critical threshold level of a product(s) (e.g. p21/waf1) by subsequent injury or related stresses to score a function.

Here, we have tried to correlate transcriptional changes with cell cycle events using a cell separation technique such as centrifugal elutriation. Elutriation, unlike general cell cycle inhibitors, does not disturb the physiology of the cell and therefore is a reliable method of isolating cells from various stages of the cell cycle. Interestingly, gamma irradiation treatment blocked the Tax+ clone (WT) and not the Tax+ clone (703) CREB mutant G0/G1 cells (Fig. 5B), implying that wildtype Tax, achieved the G1/S block by increasing cdk inhibitor levels, such as p21/waf1 and p16/ink4a, both of which regulate Rb phosphorylation. However, when S and G2/M fractionated WT cells were gamma irradiated, they clearly apoptosed. This was not evident in the 703 CREB mutant S or G2/M cells. Again, this implies that depending on which stage of the cell cycle the cells are in, they would respond very differently to injury. Results from the CREB mutant line also implies that the Tax/CREB/PCAF interaction/pathway is important for both the G1/S checkpoint block and the S and G2/M mediated apoptosis.

We also have inquired about the role of p53 in the G2/M cell cycle checkpoint in HTLV-1 and/or Tax expressing cells. Reduced or absent levels of a functional p53 in WT Tax expressing cells (as seen with any HTLV-1 infection) correlates well with increased G2/M phase arrest, micronucleation, and p53-independent irradiation-induced apoptosis. Positive control surviving cells with intact p53 (MOLT-4 cells used in this study) progress through mitosis and transiently accumulate in the G1 phase, coincident with increased p53 and p21/waf1 protein levels. The morphological appearance of the p53-independent apoptosis in WT cells suggests that death may have arisen as the result of aberrant mitosis. Data presented here supports the idea that a p53-independent, G2/M apoptotic mechanism permits the engagement of apoptosis, probably by a mitotic catastrophe, after 7.7 Gy of γ -irradiation.

14-3-3 proteins are novel types of adapter proteins that modulate interactions between components involved in signal transduction pathway and cell cycle control. Specifically, they control cytoplasmic events at G2/M and are responsible for initiating a block or loss of checkpoint at the G2/M phase. When we checked the levels of 14-3-3 in any Tax expressing cells with or without irradiation, we observed no apparent dramatic changes in the protein levels. However, 14-3-3 interacting proteins changed in WT cells after gamma irradiation, implying that loss of these partners (e.g. transla-

tion factors, cdc2, etc.) may initiate the apoptosis in these cells.

Recently, Pise-Masison *et al.* [71] have performed a series of microarray experiments characterizing the differential gene expression profile of HTLV-1-transformed (C81 and HUT 102) and -immortalized cell lines (Bes and Champ, ATL cell lines). They have identified several response pathways involving G2/M checkpoint control factors, DNA replication factors, transcriptional regulators, and kinase/phosphatase signaling molecules that are deregulated in HTLV-1-infected cells. Interestingly, they also observed similar results concerning the expression profiles of pro- and anti-apoptotic genes. Consistent with our results, Pise-Masison *et al.* found an upregulation of Bcl-xL, 14-3-3 τ , and p21/Waf1.

Concerning the deregulation of the G2/M transition, we observed a decreased binding of 14-3-3 τ interacting partners following DNA damage and concomitant apoptosis. Pise-Masison *et al.* have found the upregulation of three proteins that are involved in the G2/M transition, including Cdc25C, cyclin B, and Cdc2; which we confirmed as 14-3-3 τ interacting proteins. More importantly, they also observed the increased expression of 14-3-3 τ in both C81 and HUT 102 cell lines. Thus, the increased expression of these proteins in both C81 and HUT 102 cell lines indicate a normally regulated G2/M transition without subsequent apoptosis. However, upon the use of DNA damage-inducing agents, the G2/M checkpoint may in fact be deregulated by the loss of 14-3-3 τ partners and subsequent apoptosis, as observed in the current study.

Finally, how does pro-apoptotic initiating signals, such as 14-3-3 interacting proteins, in WT Tax expressing cells mediate communication between activated caspase-8 (Fig. 4) and the mitochondrial death (RIP, Bax, NIP3, and MKK3) machinery? Caspase-8 activation can initiate two pathways leading to the activation of downstream caspases-3, -6, and -7. Activation can occur through direct cleavage [52, 53] of these caspases. This pathway is predominant when the caspase 8 concentration is high [54]. On the other hand, caspase 8 can activate the downstream caspases indirectly by inducing cytochrome C release from the mitochondria that triggers caspase activation through Apaf-1. The indirect pathway, mediated by Bid and dependent on cytochrome C release, represents an important amplification step in the presence of low caspase 8 concentration.

Extensive studies have demonstrated that the Bcl-2 family of proteins can positively and negatively regulate apoptosis [55–59]. Intriguingly, the Bcl-2 family possess anti-apoptotic (Bcl-2, Bcl-x_L, Bcl-W, Bag-1, Mcl-1, and A1/Bfl-1) as well as pro-apoptotic (Bad, Bax, Bak, Bcl-x_s, Bid, Bik, Hrk) molecules [56, 57, 60].

In mammalian cells, apoptosis can be inhibited by overexpression of anti-apoptotic members of the Bcl-2 family,

including Bcl-2, Bcl-xL, MCL-1, Bcl-w and Bfl-1. Overexpression of Bcl-2 or Bcl-xL blocks cytochrome C release in response to a variety of apoptotic stimuli [61–64]. Several domains of the Bcl-2 family proteins, Bcl-2 homology (BH) domains, are evolutionarily conserved. BH1 and BH2 domains are common throughout the family for anti-apoptotic members [65, 66]. Bfl-1 is the smallest member of the Bcl-2 family and has been shown to retard apoptosis and permit proliferation in various cell lines [48–67]. Mutational analysis of the *bfl-1* gene has revealed that mutations within the BH1 and BH2 domains abolished the anti-apoptotic activity, whereas the N-terminal domain contributed to the proliferative activity of Bfl-1 [67].

When examining for expression of Bcl-2 family members, we observed higher levels of Bfl-1 in CREB mutant 703 cells. This may be due to the trans-dominance of the Tax/NF κ B pathway and may contribute to the overall expression of Bcl-2 family members resulting in loss of G1/S checkpoint and lack of apoptosis in these cells. Importantly, the Bfl-1 gene contains a consensus NF κ B sequence in its promoter which was responsive to wildtype and mutant (M47) Tax, but not to the mutant (M22) Tax, implying that the NF κ B site in the Bfl-1 promoter is the site of activated transcription by Tax. Collectively, the anti-apoptotic phenotype of the CREB mutant Tax implies that inhibition of NF κ B activation could serve as an excellent target for inhibiting the growth of HTLV-1 infected cells.

Finally, an important implication from this study could be at the level of ATL and HAM/TSP patient treatment. Effectiveness of DNA damaging agents and drugs targeting virally infected cells may be determined by which phase of the cell cycle the cells are in. As in the case of HTLV-1, the response of the viral activator Tax to cellular stress was determined by the cell cycle phase in which they were targeted (Fig. 5A). If G1 cells were hit with a DNA damaging agent, such as gamma irradiation, they blocked efficiently at the G1/S checkpoint through the transcriptional upregulation of p21/waf1, p16/ink4a, and IL-10. While S and G2/M cells underwent two distinct responses after DNA damage, the first being the loss of 14-3-3 τ 's binding partners that are involved in translational and G2/M checkpoint control, and second increase in transcription and activation of pro-apoptotic genes, such as caspases -8, -3, and -10, Bax, and MKK3, leading to apoptosis. Very important to viral replication, we have observed active viral replication and release in the G2 and G2/M phases of the cell cycle, and no viral release from the G1/S blocked population when cells were treated with γ -irradiation. This simply implies that a true treatment of HTLV-1 infected cells would need to occur somewhere within the G1 phase of the cell cycle. Current studies using cell cycle inhibitors following viral activation leads us to believe that this may be a general finding in many HTLV-1 infected cells.

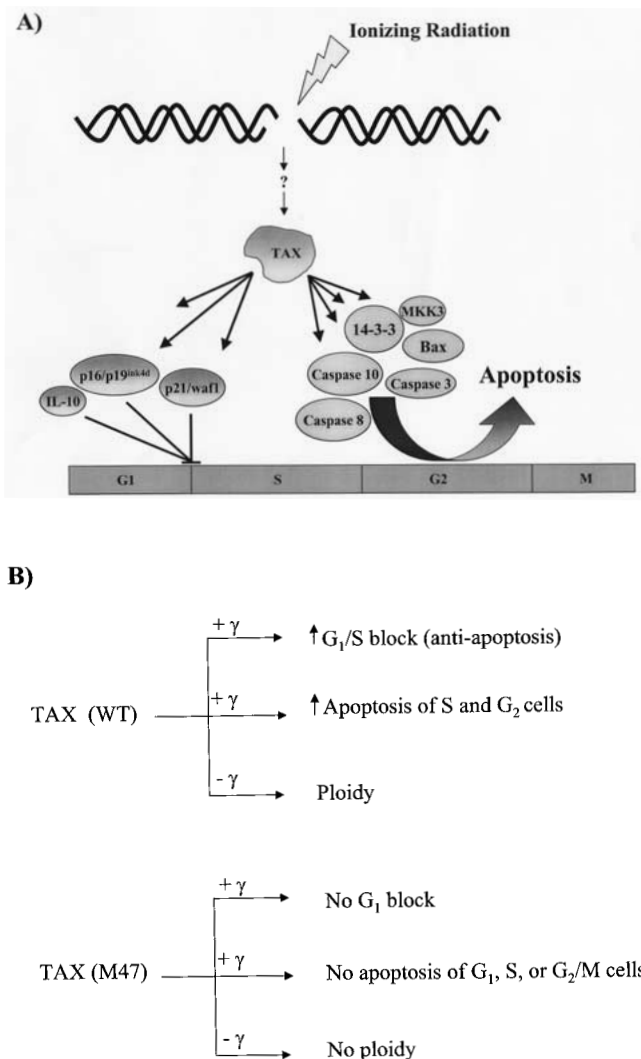


Fig. 5. Tax upregulation of various factors associated either with a G1/S block or S/G2 apoptosis upon DNA damage. (A) When Tax expressing G1 cells are treated with a DNA damaging agent, such as γ -irradiation, they block at the G1/S checkpoint through the transcriptional upregulation of p21/waf1, p16/ink4a, and IL-10. While S and G2/M cells undergo loss of 14-3-3 τ 's binding partners and subsequently increase in transcription and activation of pro-apoptotic genes, such as caspases -8, -3, and -10, Bax, and MKK3 leading to apoptosis. (B) A general diagram of cells responding to irradiation when expressing wild type or CREB mutant (M47) Tax. Wild Tax containing cells have G1/S block and increase of apoptosis from S and G2/M cells. These cells also show ploidy as a large heavy fraction when using elutriation (de la Fuente, unpublished results). Mutant Tax expressing cells show no block or apoptosis from G1, S or G2/M population and no ploidy.

Acknowledgements

We would like to thank Dr. John Brady (NIH, Bethesda, MD, USA) for supplying us with the MOLT-4 cell line, Dr. Lawrence Harrison (UMDNJ, Newark, NJ, USA) for caspase-3 and PARP antibodies, Dr. Céline Gélinas (UMDNJ-RWJMS)

for the Bfl-1 CAT and Bfl-1 mkb CAT constructs, Dr. Scott Gitlin (University of Michigan, Ann Arbor, MI, USA) for Tax polyclonal antibody, and Carolyn Eadie for her assistance in preparing this manuscript. This work was supported in part by NIH grants AI44357, AI43894 and the Alexandria and Alexander Sinsheimer foundation grant to FK and a Research Enhancement Fund (REF) from George Washington University to Dr. A. Vertes (Department of Chemistry, GWU) and FK.

References

1. Schena M, Shalon D, Davis RW, Brown PO: Quantitative monitoring of gene expression patterns with a complementary microarray. *Science* 270: 467–470, 1995
2. Lockhart DJ, Dong H, Byrne MC, Follettie MT, Gallo MV, Chee MS, Mittmann M, Wang C, Kobayashi M, Horton H, Brown EL: Expression monitoring by hybridization to high-density oligonucleotide arrays. *Nat Biotechnol* 14: 1675–1680, 1996
3. de la Fuente C, Deng L, Santiago F, Arce L, Wang L, Kashanchi F: Gene expression array of HTLV type 1-infected T cells: Up-regulation of transcription factors and cell cycle genes. *AIDS Res. Hum Retroviruses* 16: 1695–1700, 2000
4. de la Fuente C, Santiago F, Chong SY, Deng L, Mayhood T, Fu P, Stein D, Denny T, Coffman F, Azimi N, Mahieux R, Kashanchi F: Overexpression of p21^{waf1} in human T-cell lymphotropic virus type 1-infected cells and its association with cyclin A/cdk2. *J Virol* 74: 7270–7283, 2000
5. Suzuki T, Kitao S, Matsushima H, Yoshida M: HTLV-1 Tax protein interacts with cyclin-dependent kinase inhibitor p16INK4A and counteracts its inhibitory activity towards CDK4. *EMBO J.* 15: 1607–1614, 1996
6. Haller K, Ruckes T, Schmitt I, Saul D, Derow E, Grassmann R: Tax-dependent stimulation of G1 phase-specific cyclin-dependent kinases and increased expression of signal transduction genes characterize HTLV type 1-transformed T cells. *AIDS Res Hum Retroviruses* 16: 1683–1688, 2000
7. Jin DY, Spencer F, Jeang KT: Human T cell leukemia virus type 1 oncoprotein Tax targets the human mitotic checkpoint protein MAD1. *Cell* 93: 81–91, 1998
8. Santiago F, Clark E, Chong S, Molina C, Mozafari F, Mahieux R, Fuji M, Azimi N, Kashanchi F: Transcriptional up-regulation of the cyclin D2 gene and acquisition of new cyclin-dependent kinase partners in human T-cell leukemia virus type 1-infected cells. *J Virol* 73: 9917–9927, 1999
9. Van PL, Yim KW, Jin DY, Dapolito G, Kurimasa A, Jeang KT: Genetic evidence of a role for ATM in functional interaction between human T-cell leukemia virus type 1 Tax and p53. *J Virol* 75: 396–407, 2001
10. Ariumi Y, Kaida A, Lin JY, Hirota M, Masui O, Yamaoka S, Taya Y, Shimotohno K: HTLV-1 tax oncoprotein represses the p53-mediated trans-activation function through coactivator CBP sequestration. *Oncogene* 19: 1491–1499, 2000
11. Mulloy JC, Kislyakova T, Cereseto A, Casareto L, LoMonico A, Fullen J, Lorenzi MV, Cara A, Nicot C, Giam C, Franchini G: Human T-cell lymphotropic/leukemia virus type 1 Tax abrogates p53-induced cell cycle arrest and apoptosis through its CREB/ATF functional domain. *J Virol* 72: 8852–8860, 1998
12. Pise-Masison CA, Radonovich M, Sakaguchi K, Appella E, Brady JN: Phosphorylation of p53: A novel pathway for p53 inactivation in human T-cell lymphotropic virus type 1-transformed cells. *J Virol* 72: 6348–6355, 1998

13. Pise-Masison CA, Mahieux R, Radonovich M, Jiang H, Brady JN: Human T-lymphotropic virus type I Tax protein utilizes distinct pathways for p53 inhibition that are cell type-dependent. *J Biol Chem* 276: 200–205, 2001
14. Kao SY, Lemoine FJ, Mariott SJ: HTLV-1 Tax protein sensitizes cells to apoptotic cell death induced by DNA damaging agents. *Oncogene* 19: 2240–2248, 2000
15. Hall AP, Irvine J, Blyth K, Cameron ER, Onions DE, Campbell ME: Tumours derived from HTLV-1 tax transgenic mice are characterized by enhanced levels of apoptosis and oncogene expression. *J Pathol* 186: 209–214, 1998
16. Chen X, Zachar V, Zdravkovic M, Guo M, Ebbesen P, Liu X: Role of the Fas/Fas ligand pathway in apoptotic cell death induced by the human T cell lymphotropic virus type I Tax transactivator. *J Gen Virol* 78: 3277–3285, 1997
17. Chlichlia K: ICE-proteases mediate HTLV-1 Tax-induced apoptotic T-cell death. *Oncogene* 14: 2265–2272, 1997
18. Nicot C, Harrod R: Distinct p300-responsive mechanisms promote caspase-dependent apoptosis by human T-cell lymphotropic virus type I Tax protein. *Mol Cell Biol* 20: 8580–8589, 2000
19. Brauweiler A, Garrus JE, Reed JC, Nyborg JK: Repression of bax gene expression by the HTLV-1 Tax protein: Implications for suppression of apoptosis in virally infected cells. *Virology* 231: 135–140, 1997
20. Tsukahara T, Kannagi M, Ohashi T, Kato H, Arai M, Nunez G, Iwanaga Y, Yamamoto N, Ohtani K, Nakamura M, Fujii M: Induction of Bcl-x(L) expression by human T-cell leukemia virus type I Tax through NF-kappaB in apoptosis-resistant T-cell transfectants with Tax. *J Virol* 73: 7981–7987, 1999
21. Kawakami A, Nakashima T, Sakai H, Urayama S, Yamasaki S, Hida A, Tsuboi M, Nakamura H, Ida H, Migita K, Kawabe Y, Eguchi K: Inhibition of caspase cascade by HTLV-1 tax through induction of NF-kappaB nuclear translocation. *Blood* 94: 3847–3854, 1999
22. Li X, Darzynkiewicz Z: Cleavage of Poly(ADP-ribose) polymerase measured *in situ* in individual cells: Relationship to DNA fragmentation and cell cycle position during apoptosis. *Exp Cell Res* 255: 125–132, 2000
23. Dantzer F, Nasheuer HP, Vonesch JL, de Murcia G, Menissier-de Murcia J: Functional association of poly(ADP-ribose) polymerase with DNA polymerase alpha-primase complex: A link between DNA strand break detection and DNA replication. *Nucleic Acids Res* 26: 1891–1898, 1998
24. Baldin V: 14-3-3 proteins and growth control. *Prog Cell Cycle Res* 4: 49–60, 2000
25. Chan TA, Hermeking H, Lengauer C, Kinzler KW, Vogelstein B: 14-3-3 Sigma is required to prevent mitotic catastrophe after DNA damage. *Nature* 401: 616–620, 1999
26. el-Deiry WS: Regulation of p53 downstream genes. *Semin Cancer Biol* 8: 345–357, 1998
27. Kashanchi F *et al.*: In: R. Ahmed, I. Chen (eds). *Human T-cell Leukemia Virus. Persistent Viral Infections*. John Wiley and Sons Ltd., New York, 1999, pp 47–75
28. Ng PW, Iha H, Iwanaga Y, Bittner M, Chen Y, Jiang Y, Gooden G, Trent JM, Meltzer P, Jeang KT, Zeichner SL: Genome-wide expression changes induced by HTLV-1 Tax: Evidence for MLK-3 mixed lineage kinase involvement in Tax-mediated NF-kappaB activation. *Oncogene* 20: 4484–96, 2001
29. O'Connor PM: Mammalian G1 and G2 phase checkpoints. *Cancer Surv* 29: 151–182, 1997
30. Szumiel I: Monitoring and signaling of radiation-induced damage in mammalian cells. *Radiat Res* 150: S92–S101, 1998
31. Dasika GK, Lin SC, Zhao S, Sung P, Tomkinson A, Lee EY: DNA damage-induced cell cycle checkpoints and DNA strand break repair in development and tumorigenesis. *Oncogene* 18: 7883–7899, 1999
32. Liu Q, Guntuku S, Cui XS, Matsuoka S, Cortez D, Tamai K, Luo G, Carattini-Rivera S, DeMayo F, Bradley A, Donehower LA, Elledge SJ: Chk1 is an essential kinase that is regulated by Atr and required for the G(2)/M DNA damage checkpoint. *Genes Dev* 14: 1448–1459, 2000
33. Hirao A, Kong YY, Matsuoka S, Wakeham A, Ruland J, Yoshida H, Liu D, Elledge SJ, Mak TW: DNA damage-induced activation of p53 by the checkpoint kinase Chk2. *Science* 287: 1824–1827, 2000
34. Waldman T, Kinzler KW, Vogelstein B: p21 is necessary for the p53-mediated G1 arrest in human cancer cells. *Cancer Res* 55: 5187–5190, 1995
35. Fernandez J, Gharahdaghi F, Mische SM: Routine identification of proteins from sodium dodecyl sulfate-polyacrylamide gel electrophoresis (SDS-PAGE) gels or polyvinylidene difluoride membranes using matrix assisted laser desorption/ionization-time of flight-mass spectrometry (MALDI-TOF-MS). *Electrophoresis* 19: 1036–1045, 1998
36. Harhaj EW, Good L, Xiao G, Sun SC: Gene expression profiles in HTLV-1-immortalized T cells: deregulated expression of genes involved in apoptosis regulation. *Oncogene* 18: 1341–1349, 1999
37. Thullberg M, Bartkova J, Khan S, Hansen K, Ronnstrand L, Lukas J, Strauss M, Bartek J: Distinct vs. redundant properties among members of the INK4 family of cyclin-dependent kinase inhibitors. *FEBS Lett* 470: 161–166, 2000
38. Biolo G, Bosutti A, Iscra F, Toigo G, Gullo A, Guarnieri G: Contribution of the ubiquitin-proteasome pathway to overall muscle proteolysis in hypercatabolic patients. *Metabolism* 49: 689–691, 2000
39. Saeki K, Yuo A, Suzuki E, Yazaki Y, Takaku F: Aberrant expression of cAMP-response-element-binding protein ('CREB') induces apoptosis. *Biochem J* 343: 249–255, 1999
40. Trucco C, Oliver FJ, de Murcia G, Menissier-de Murcia J: DNA repair defect in poly(ADP-ribose) polymerase-deficient cell lines. *Nucleic Acids Res* 26: 2644–2649, 1998
41. Dantzer F, Schreiber V, Niedergang C, Trucco C, Flatter E, De La Rubia G, Oliver J, Rolli V, Menissier-de Murcia J, de Murcia G: Involvement of poly(ADP-ribose) polymerase in base excision repair. *Biochimie* 81: 69–75, 1999
42. Yakovlev AG, Wang G, Stoica BA, Simbulan-Rosenthal CM, Yoshihara K, Smulson ME: Role of DNAS1L3 in Ca²⁺- and Mg²⁺-dependent cleavage of DNA into oligonucleosomal and high molecular mass fragments. *Nucleic Acids Res* 27: 1999–2005, 1999
43. Gong B, Almasan A: Differential upregulation of p53-responsive genes by genotoxic stress in hematopoietic cells containing wild-type and mutant p53. *Gene Expr* 8: 197–206, 1999
44. Chen F, Wagner PD: 14-3-3 proteins bind to histone and affect both histone phosphorylation and dephosphorylation. *FEBS Lett* 347: 128–132, 1994
45. Waterman MJ, Stavridi ES, Waterman JL, Halazonetis TD: ATM-dependent activation of p53 involves dephosphorylation and association with 14-3-3 proteins. *Nat Genet* 19: 175–178, 1998
46. Wang S, Miura M, Jung YK, Zhu H, Li E, Yuan J: Murine caspase-11, an ICE-interacting protease, is essential for the activation of ICE. *Cell* 92: 501–509, 1998
47. Budihardjo I, Oliver H, Lutter M, Luo X, Wang X: Biochemical pathways of caspase activation during apoptosis. *Annu Rev Cell Dev Biol* 15: 269–290, 1999
48. D'Sa-Eipper C, Chinnadurai G: Functional dissection of Bfl-1, a Bcl-2 homolog: Anti-apoptosis, oncogene-cooperation and cell proliferation activities. *Oncogene* 16: 3105–3114, 1998
49. Chen C, Edelstein LC, Gelinas C: The Rel/NF-kappaB family directly activates expression of the apoptosis inhibitor Bcl-x(L). *Mol Cell Biol* 20: 2687–2695, 2000
50. Zong WX, Edelstein LC, Chen C, Bash J, Gelinas C: The prosurvival Bcl-2 homolog Bfl-1/A1 is a direct transcriptional target of NF-kappaB that blocks TNF alpha-induced apoptosis. *Genes Dev* 13: 382–387, 1999

51. Nicot C, Mahieux R, Takemoto S, Franchini G: Bcl-X(L) is up-regulated by HTLV-I and HTLV-II *in vitro* and in *ex vivo* ATLL samples. *Blood* 96: 275–281, 2000
52. Muzio M, Chinnaiyan AM, Kischkel FC, O'Rourke K, Shevchenko A, Ni J, Scaffidi C, Bretz JD, Zhang M, Gentz R, Mann M, Krammer PH, Peter ME, Dixit VM: FLICE, a novel FADD-homologous ICE/CED-3-like protease, is recruited to the CD95 (Fas/APO-1) death-inducing signaling complex. *Cell* 85: 817–827, 1996
53. Srinivasula SM, Ahmad M, Fernandes-Alnemri T, Litwack G, Alnemri ES: Molecular ordering of the Fas-apoptotic pathway: The Fas/APO-1 protease Mch5 is a CrmA-inhibitable protease that activates multiple Ced-3/ICE-like cysteine proteases. *Proc Natl Acad Sci USA* 93: 14486–14491, 1996
54. Kuwana T, Smith JJ, Muzio M, Dixit V, Newmeyer DD, Kornbluth S: Apoptosis induction by caspase-8 is amplified through the mitochondrial release of cytochrome c. *J Biol Chem* 273: 16589–16594, 1998
55. Adams JM, Cory S: The Bcl-2 protein family: Arbiters of cell survival. *Science* 281: 1322–1326, 1998
56. Chao DT, Korsmeyer SJ: BCL-2 family: Regulators of cell death. *Annu Rev Immunol* 16: 395–419, 1998
57. Reed JC: Double identity for proteins of the Bcl-2 family. *Nature* 387: 773–776, 1997
58. Reed JC: Bcl-2 family proteins. *Oncogene* 17: 3225–3236, 1998
59. Thompson CB: Apoptosis in the pathogenesis and treatment of disease. *Science* 267: 1456–1462, 1995
60. Wang CY, Guttridge DC, Mayo MW, Baldwin AS Jr: NF-kappaB induces expression of the Bcl-2 homologue A1/Bfl-1 to preferentially suppress chemotherapy-induced apoptosis. *Mol Cell Biol* 19: 5923–5929, 1999
61. Kluck RM, Bossy-Wetzel E, Green DR, Newmeyer DD: The release of cytochrome c from mitochondria: A primary site for Bcl-2 regulation of apoptosis. *Science* 275: 1132–1136, 1997
62. Vander Heiden MG, Chandel NS, Williamson EK, Schumacker PT, Thompson CB: Bcl-xL regulates the membrane potential and volume homeostasis of mitochondria. *Cell* 91: 627–637, 1997
63. Scaffidi C, Fulda S, Srinivasan A, Friesen C, Li F, Tomaselli KJ, Debatin KM, Krammer PH, Peter ME: Two CD95 (APO-1/Fas) signaling pathways. *EMBO J* 17: 1675–1687, 1998
64. Zhang H, Cowan-Jacob SW, Simonen M, Greenhalf W, Heim J, Meyhack B: Structural basis of BFL-1 for its interaction with BAX and its anti-apoptotic action in mammalian and yeast cells. *J Biol Chem* 275: 11092–11099, 2000
65. Oltvai ZN, Millman CL, Korsmeyer SJ: Bcl-2 heterodimerizes *in vivo* with a conserved homolog, Bax, that accelerates programmed cell death. *Cell* 74: 609–619, 1993
66. Kelekar A, Thompson CB: Bcl-2-family proteins: The role of the BH3 domain in apoptosis. *Trends Cell Biol* 8: 324–330, 1998
67. D'Sa-Eipper C, Subramanian T, Chinnadurai G: bfl-1, a bcl-2 homologue, suppresses p53-induced apoptosis and exhibits potent cooperative transforming activity. *Cancer Res* 56: 3879–3882, 1996
68. Salahuddin SZ, Markham PD, Wong-Staal F, Franchini G, Kalyanaraman VS, Gallo RC: Restricted expression of human T-cell leukemia-lymphoma virus (HTLV) in transformed human umbilical cord blood lymphocytes. *Virology* 129: 51–64, 1983
69. Bhat NK, Adachi Y, Samuel KP, Derse D: HTLV-1 gene expression by defective proviruses in an infected T-cell line. *Virology* 196: 15–24, 1993
70. Lacoste J, Petropoulos L, Pepin N, Hiscott J: Constitutive phosphorylation and turnover of I kappa B alpha in human T-cell leukemia virus type I-infected and Tax-expressing T cells. *J Virol* 69: 564–569, 1995
71. Pise-Masison CA, Radonovich M, Mahieux R, Chatterjee P, Whiteford C, Duvall J, Guillerm C, Gessain A, Brady JN: Transcription profile of cells infected with human T-cell leukemia virus type I compared with activated lymphocytes. *Cancer Res* 62: 3562–3571, 2002

